

*George R. Town*

# HAZELTINE SERVICE CORPORATION

(A SUBSIDIARY OF HAZELTINE CORPORATION)

NEW YORK LABORATORY:  
333 West 52nd Street  
Columbus 5-0793

CHICAGO LABORATORY:  
325 West Huron Street  
Superior 0790

BAYSIDE LABORATORY:  
Bayside, Long Island.  
FLushing 7-5300

This Report is the property of the Hazeltine Service Corporation and is prepared for the exclusive use of its authorized representatives.

*Report No. 1945*

TITLE      **MAGNETIC SCANNING COILS**  
                  **(TELEVISION PRINCIPLES - CHAPTER 11)**

DATE      *April 28, 1939.*

MFR.      *General.*

*STROBER-GULLICK INC. N.Y.C.*

Approved *W. A. Mac Donald*

This report gives the result of investigations by our engineers. Use of the information herein contained is on the sole responsibility of the recipient of the report. No recommendations are made by the Company and no responsibility is assumed by the Company. The report is forwarded to you for your information only. It is not for general distribution and should be treated as confidential.  
HAZELTINE SERVICE CORPORATION

MAGNETIC SCANNING COILS  
(TELEVISION PRINCIPLES - CHAPTER 11)

C. E. Dean  
Editor

TABLE OF CONTENTS

	<u>Page</u>
INTRODUCTION - - - - -	245
DESCRIPTION OF VARIOUS TYPES OF SCANNING COILS - -	245
Arrangements of Windings - - - - -	245
Iron Sheaths - - - - -	246
FACTORS GOVERNING COIL DIAMETER AND LENGTH - - -	248
THE CONCENTRATED TYPE OF SCANNING COIL - - -	250
Computation of Field Strength - - - - -	250
Optimum Separation of Windings of Concentrated Coil -	251
DISTRIBUTED TYPE OF SCANNING COIL - - - - -	252
TESTING OF SCANNING COILS - - - - -	254
Energy Factor - - - - -	254
Power-Dissipation Factor - - - - -	255
Measurement of Field Intensity - - - - -	256
Measurement of Sawtooth Currents - - - - -	258
Testing for Uniformity of Scanning Speed - - -	259
TRANSFORMERS FOR SCANNING COILS - - - - -	263
Reasons for Using a Transformer - - - - -	263
Design of Line-Frequency Transformers - - - - -	264
Attenuation of Line Transformer - - - - -	266
Efficiency of Line Transformer - - - - -	266
Resistance in Line-Transformer Circuits - - - - -	267
Field-Frequency Transformer - - - - -	267
EFFECT OF HYSTERESIS IN IRON - - - - -	267
REFERENCES - - - - -	267
* * * *	
TABLE I - VALUES OF ENERGY FACTOR $q$ AND ENERGY-DISSIPATION FACTOR $p$ FOR LINE AND FIELD COILS OF SEVERAL YOKES	257
* * * *	

SPECIFICATIONS SELECTED FROM  
THIS CHAPTER

Usual External Diameter of Glass Neck of Magnetically Scanned Picture Tubes -	- 35 Millimeters
Character of Impedance of Line Scanning Coil for 13,230-Cycle Sawtooth Currents - - - - -	Mainly Inductive
Representative Inductance of Line Scanning Coil (Consisting of Two Windings in Series and Designed for Operation with Transformer) -	1.5 Millihenries
Character of Impedance of Field Scanning Coil for 60-Cycle Saw- tooth Currents - - - - -	Mainly Resistive
Representative Direct-Current Resistance of Field Scanning Coil Designed for Operation with Transformer - - - - -	20 Ohms
Same Except Coil Designed for Direct Operation - - - - -	5000 Ohms
Factor by Which to Multiply Reading of Thermal Meter on Sawtooth Wave to Get Peak-to-Peak Value - - - - -	3.46
Factor by Which to Multiply Reading of Rectifier-Type Meter on Sawtooth Wave to Get Peak-to-Peak Value (Use such a meter only on field-frequency waves) - - - - -	3.60

\* \* \* \*

## MAGNETIC SCANNING COILS

### (TELEVISION PRINCIPLES - CHAPTER 11)

#### INTRODUCTION

In the preceding chapter a general description of the scanning process in a magnetically scanned picture tube is given. The relation between the magnetic deflecting flux density and the angle of deflection of the cathode-ray beam is developed, and the energy in the magnetic field is discussed. The relations between these factors and the beam voltage, as well as the length of the deflecting coil and the internal tube-neck diameter, are also developed.

The purpose of the present chapter is to examine the scanning coils in more detail from the standpoints of design and performance. A number of different practical coil designs are discussed and for several of these the relations between the ampere-turns of the coil and the magnetic field intensity in the scanning zone of the coil are developed. The use of iron sheaths with scanning coils is discussed.

Scanning coils are frequently coupled to the vacuum-tube driving circuit thru a transformer. The design of such transformers is also discussed in the present chapter, and formulas for matching of the input and output impedances are developed.

Methods of testing scanning coils under normal sawtooth-current excitation are described. One method makes use of a pickup coil which is placed within the scanning coil. The voltage induced in this coil, after clipping of the retrace impulses and suitable amplification, is examined with a cathode-ray oscilloscope to determine the degree of linearity of the scanning wave.

A great deal of the discussion which follows applies equally to horizontal (or line) scanning and to vertical

(or field) scanning, so that the term "scanning coil" is used to describe either type. In general, for simplification, only one of these is shown in the drawings. Where the discussion is applicable to only one direction, the term "line scanning coil" or "field scanning coil" is used.

It is common practice to have the same scanning center for both the line and the field scanning coils. In this design, the field scanning coil is placed around the outside of the line scanning coil. Each coil has whatever wire size and number of turns are best adapted to its own circuit conditions. It is possible to produce horizontal and vertical magnetic scanning fields in the same region, since the presence of one coil does not distort the field from the other. When the two pairs of scanning coils are placed accurately at right angles, the inductive coupling between them is balanced out. There is a residual capacitive coupling whose effect is discussed later. (In the case of electrostatic scanning, the two scanning fields may not be superposed, since one pair of deflecting plates, being equipotential surfaces, cannot be brought close to the other pair without causing distortion of both fields.)

#### DESCRIPTION OF VARIOUS TYPES OF SCANNING COILS

##### Arrangements of Windings

Figure 1 shows a simple type of coil consisting of a pair of windings, adapted to be located on opposite sides of the neck of a tube. Each winding consists of straight longitudinal portions and curved end portions. That is, the end portions are bent into circular arcs lying in a plane normal to the electron-

optical axis. The magnetic field from the end portion of one winding approximately neutralizes that from the adjacent end portion of the other winding, so that one can consider the field from this coil, with its two windings, as approximately that produced by the longitudinal conductors alone. In the next section, on page 250, we show the relation between the field strength at the center of such a coil and the spacing of the conductors. The term "concentrated coil" is used hereafter to indicate this type.

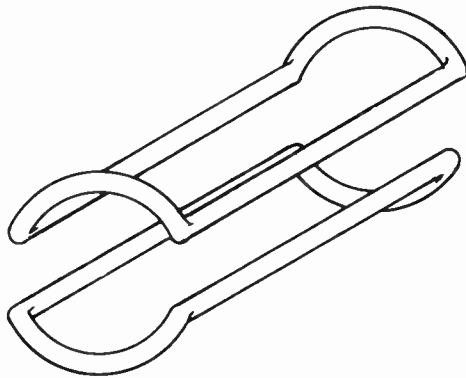


Fig. 1. Concentrated Type of Scanning Coil.

A more uniform field strength throughout the scanning zone can be obtained by distributing the longitudinal conductors in the manner shown in Figure 2. The term "distributed coil" is used hereafter to indicate this type.

A third type of coil, which is frequently used, is illustrated in Figure 3. This type of coil lends itself well to mechanical construction since the end portions are not bent away from the coil but lie on a cylindrical surface. The term "nested coil" is applied to this type.

In each of these coil types the field at the end of the coil does not drop abruptly to zero, but follows a more or less sharp transition. This transition or fringing field produces some distortion in the deflected electron beam, so that it is important to minimize it.

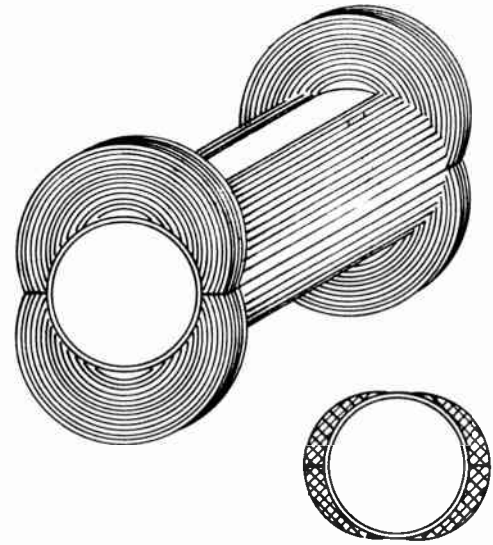


Fig. 2. Distributed Type of Scanning Coil.

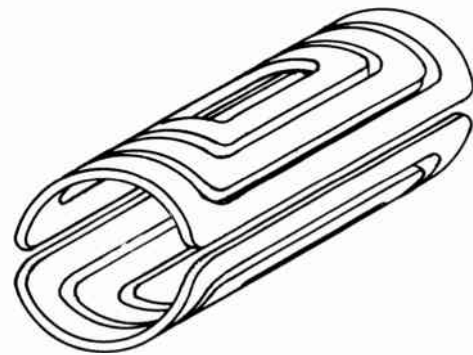


Fig. 3. Nested Type of Scanning Coil.

#### Iron Sheaths

The coils described above may be operated as air-core coils. In this mode of operation, the magnetic return flux fills a large volume, as is illustrated in Figure 4, which shows the magnetic field in a cross-section of the

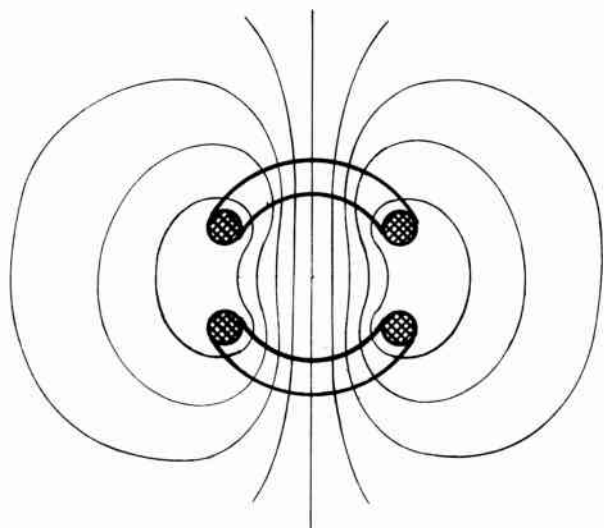


Fig. 4. Flux Lines of Concentrated Coil with Air Core.

concentrated coil of Figure 1. The only part of the magnetic field which is useful is that in the scanning zone within the coil. The external return flux is objectionable for the following reasons: (1) its energy represents about half the total magnetic field energy, which is thus wasted; (2) it permits coupling of the scanning field to external parts of the circuits so that these parts must be shielded or placed at a distance; and (3) it disturbs the field at the ends of the coil, thus contributing to the fringing field.

The external or return field may be modified by surrounding the coil with a laminated-iron cylindrical shell or sheath. In the case of a concentrated coil, the resulting field is as shown in Figure 5. The presence of the sheath improves the coil in each of the three respects mentioned in the preceding paragraph, namely: (1) a greater portion of the total energy in the magnetic field is located in the scanning zone; (2) the coil is magnetically less coupled with external parts of the circuit; and (3) the fringing field at the ends of the coil drops off more abruptly.

This iron sheath may be made up in a number of ways, each designed to

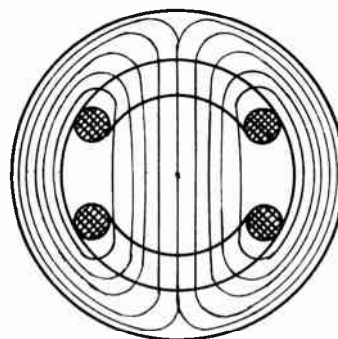


Fig. 5. Flux Lines of Concentrated Coil with Iron Sheath.

minimize eddy currents. For example, it may be made up of iron wire of small diameter which is wound in a cylindrical helix of several layers on the outside of the scanning coil, as shown in Figure 6.

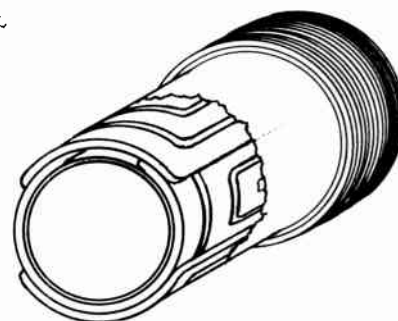


Fig. 6. Scanning Yoke with Iron-Wire Sheath.

In another construction the sheath is made up of thin flat iron laminations which are in the form of rings having a hole of such size that they fit over the outside of the scanning coil; these rings are perpendicular to the tube axis. This type is shown in Figure 7.

The iron wire or laminations should of course be thin, and the adjacent surfaces insulated by varnish or oxide, according to transformer practice.

In another construction the magnetic return path consists of an iron

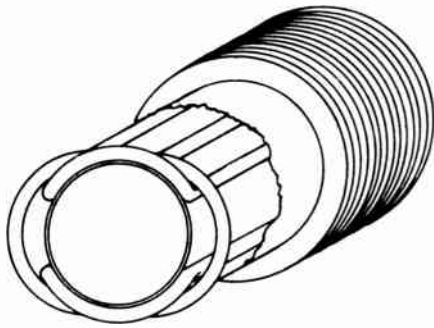


Fig. 7. Scanning Yoke with Laminated-Iron Sheath.

sheath having slots in which the coils are wound, as in motor practice. If both line and field scanning coils are wound on the same structure, the number of slots or poles must be some multiple of 4. Figure 8 shows an example of this type of iron sheath, having 12 slots, which resembles an induction-motor winding. In this arrangement the turns of each coil are so distributed that the magnetic field produced in the scanning zone is uniform. One type of winding distribution is shown schematically for a single coil. (A photograph and description of a scanning coil of this type are given on pages 273-274 of "Electron Optics in Television", by Maloff and Epstein.)

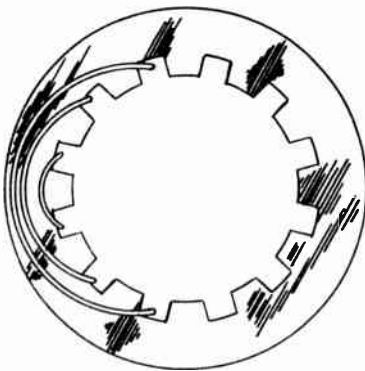


Fig. 8. Slotted Laminated-Iron Sheath with Diagrammatic Representation of One Winding.

Where line and field scanning coils are placed at different positions along the axis of the tube, the line scanning coil may be of one of the types described, placed at the neck of the tube. The field scanning coil in this case may be a two-pole iron-core type of the shape shown in Figure 9, which is designed to be placed on the conical bulb closer to the screen than the line scanning coil. Since this type of field scanning coil has a large air gap and must fill a correspondingly large volume of scanning zone with the magnetic field, its efficiency is comparatively low.

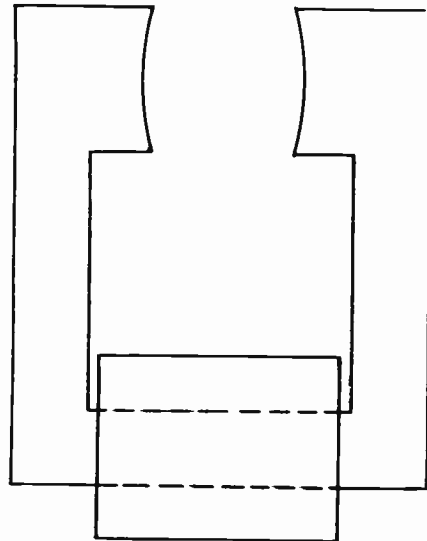


Fig. 9. Separate Yoke for Vertical Scanning.

FACTORS GOVERNING COIL  
DIAMETER AND LENGTH

In the preceding chapter on pages 232-233 the relation between the scanning-coil length, the tube internal neck diameter, and the maximum scanning angle of the cathode-ray beam is shown to be

$$\frac{A}{L} = 2 \tan \frac{\Phi}{2},$$

where  $A$  = effective internal diameter of tube neck;

$L$  = maximum usable length  
of scanning coil; and  
 $\bar{\theta}$  = maximum deflection angle.

We see from the above equation that the maximum scanning angle  $\bar{\theta}$  depends on the ratio of  $A$  and  $L$ , so that if the effective internal neck diameter  $A$  is reduced,  $L$  may be reduced in the same proportion without affecting  $\bar{\theta}$ . The reduction of  $A$  and  $L$  by a factor, say a fraction  $K$ , will reduce the volume of the magnetic scanning field by a factor  $K^3$ . Since the length of the scanning zone is diminished by the factor  $K$ , the field intensity must be increased by the factor  $1/K$  to obtain the same deflection as before, which means that the energy density in the field is increased by a factor  $1/K^2$ . Accordingly, the energy in the field is reduced by a factor  $K^3/K^2$ , or  $K$ . For example, if the dimensions of the scanning coils are halved, the required scanning energy is reduced to only half of its previous value. Such a decrease in scanning-coil size appears to offer a desirable saving in scanning power, but there is the drawback that the distortion in the deflected beam is increased. This occurs because the cross-sectional width of the cathode-ray beam, which is predetermined, becomes a greater fraction of the diameter  $A$  as the latter is diminished, so that the distortion of the beam due to the fringing field increases. In addition, a reduction in the scanning-coil internal diameter beyond the nominal glass-tube neck size requires a constriction of the glass neck at the scanning zone and a separable scanning-coil assembly. Present practice makes use of a solid scanning-coil unit, thru which the base end of the tube passes.

It should also be noted that the volume of the scanning zone swept out by the scanning beam has something of a pyramidal shape, the apex being at the entrance of the beam into the scanning field and the base being at the exit of the beam from the scanning field. The fringing field at the end of the coil where the beam enters is therefore of no consequence and does not produce defocus of the beam. It is possible to decrease the volume of the scanning field by tapering the neck of the tube and using tapered

scanning coils, such as illustrated in Figure 10. This construction requires a constriction in the glass tube and a separable scanning-coil assembly, but maintains the ratio between the beam diameter and the internal neck diameter  $A$  at the exit of the beam, which is not true for the preceding case characterized by a uniform reduction of dimensions by the factor  $K$ .

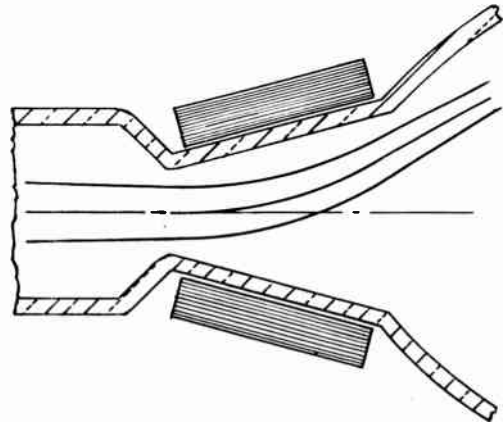


Fig. 10. Tapered Scanning Coil.

Figure 11 shows that the effective internal diameter  $A$  is smaller than the external diameter  $A_1$  of the glass neck of the tube. The value of  $A_1$  must exceed  $A$  by at least the width of the cathode-ray beam plus twice the thickness of the glass wall.

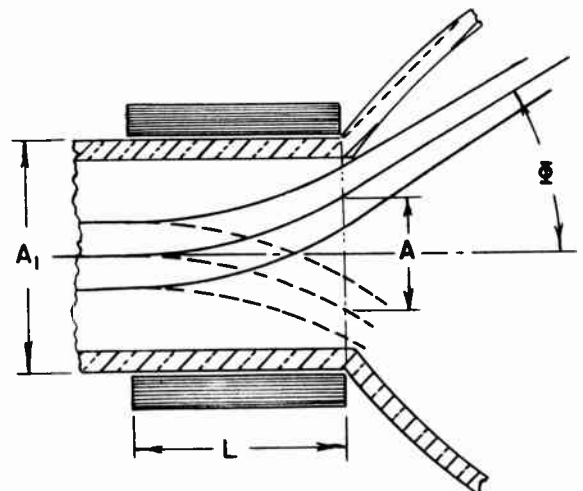


Fig. 11. Limitation of Beam Deflecting Angle by Neck Size of Tube.

For most magnetically scanned tubes the magnitude of  $A_1$ , the external neck diameter, is 35 millimeters (1.38 inches). The maximum scanning-coil length which can be used depends on the maximum scanning angle  $\Phi$ , which is measured from the undeflected position and varies from 16 degrees to 30 degrees for various tube designs. Figure 12 shows the relation between  $\Phi$  and the maximum coil length  $L$ , for a tube having an external neck diameter  $A_1$  of 35 millimeters, a beam diameter of 5 millimeters, and a glass-wall thickness of 2 millimeters. These dimensions give a value of  $A$  equal to 26 millimeters.

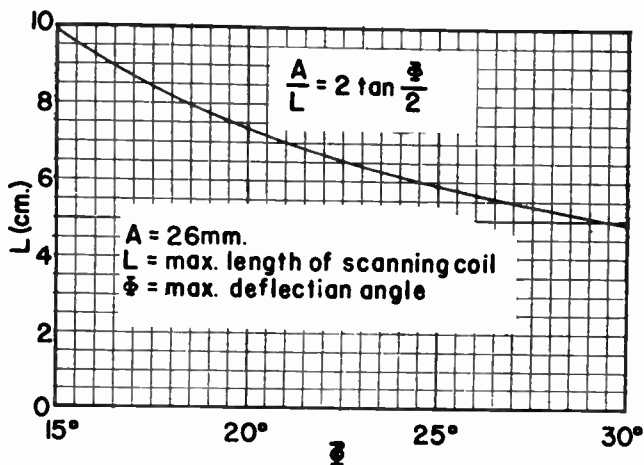


Fig. 12. Relation between Maximum Deflection Angle and Maximum Coil Length in a Practical Case.

#### THE CONCENTRATED TYPE OF SCANNING COIL

##### Computation of Field Strength

The field strength produced by some of the scanning-coil types described above can be computed for the air-core condition, if the effects of the end portions and fringing are ignored.

Figure 13 shows a cross-section of a concentrated coil, taken in a plane perpendicular to the tube axis. Characters 1 and 2 indicate cross-sections of the longitudinal conductors of the upper

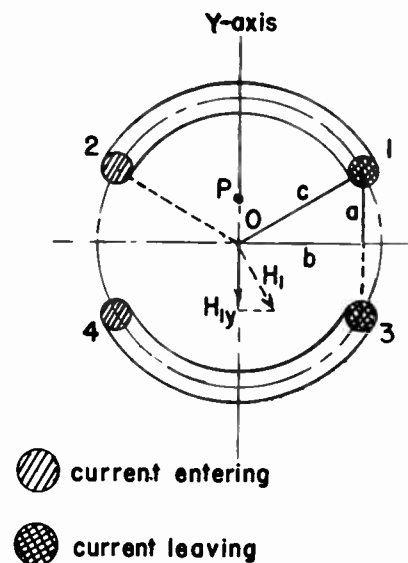


Fig. 13. Cross-Section of Concentrated Coil Taken Normal to Tube Axis.

winding, and characters 3 and 4 similarly of the lower winding. The rounded portions at the top and bottom are the end portions located at the far end of the structure as viewed. Since the diameter of any one of these cross-sections is small in comparison with the general dimensions, the individual turns of wire may be said to be concentrated, whence the name "concentrated coil" for this type. The four groups of longitudinal conductors lie on the boundary of a cylinder whose center is at point  $O$  and whose radius is  $c$ . It may be seen that  $b$  is half the width of either winding so that  $2b$  is the total width. Similarly  $a$  is half the separation between windings, so that  $2a$  is the total separation.

Should we neglect the effect of the end portions of the windings, the magnetic field at the point  $O$  is assumed to be due only to the longitudinal conductors of the coil. The direction of the field at this point is perpendicular to the plane determined by the longitudinal conductors of either the upper or lower winding. With the current entering and leaving the conductors as shown in the drawing, the direction of the field is downward.

It is advantageous to consider first the magnetic field at point O due only to the group of conductors designated 1 in the figure. The amount and direction of the field due to these conductors is indicated by the vector  $H_1$ . The amount of this field intensity is

$$H_1 = \frac{2nI}{c}, \text{ - - - - - (1) (e.m.u.)}$$

where  $H_1$  = magnetic field strength;  
 n = number of wires;  
 I = current thru each wire; and  
 c = distance from point O to center of group of wires.

The field intensity produced by the first group of conductors has a component along the y-axis, (which is taken vertically in the drawing), and this component is indicated as  $H_{1Y}$ . The magnitude of this component is less than  $H_1$  in the ratio  $b/c$ , whence from equation (1) we obtain

$$H_{1Y} = \frac{2nIb}{c^2}.$$

The total field  $H_0$  at O due to the four groups of conductors is four times this amount, since the components perpendicular to the y-axis cancel one another. The value of  $H_0$  is therefore

$$H_0 = \frac{8nIb}{c^2} . \text{ - - - - - (2) (e.m.u.)}$$

In practical units this becomes

$$H_0 = \frac{0.8nIb}{c^2}, \text{ - - - - - (3) (p)}$$

where  $H_0$  = magnetic field strength in oersteds at scanning-zone axis;  
 n = number of turns in each winding;  
 I = current thru windings in amperes;  
 b = half of width of coil in centimeters; and  
 c = radius of cylinder in centimeters.

In an ideal coil the field strength is  $H_0$  for the length L of the coil, and zero beyond this. In actual coils the field is quite uniform in the central portion but falls off more or less gradually at the ends. In the derivation of the equation for the deflection of the beam an ideal coil is assumed. If with an actual coil,  $H_0$  from equation (2) or (3) is used for the value of field strength in the deflection equation, and the length of the field is taken as the length of the coil, the computed deflection will differ slightly from the measured value. However, it has been shown experimentally that even when the length of the coil is as short as 1.5 times its diameter, the agreement between the measured and computed beam deflections is within three percent. (This result is from "Die Ablenkung des Elektronenstrahls in Braunschens Röhren mittels magnetischer Spulenfelder" by Herbert Bähring in FERNSEH A.G., December 1938, pages 15-19 or (re-numbered) 51-55.)

Optimum Separation of Windings of Concentrated Coil

The magnetic field of the concentrated coil of Figure 13 is directed along the y-direction at any point on the y-axis (say point p), but will vary in magnitude as the position of this point is changed. It is desirable to choose a value of  $a/b$  such that this gradient of the field is a minimum at point O. This will occur when the first derivative of the field has a minimum value, which is when its second derivative is zero.

Returning to equation (2), we notice that this gives  $H_0$ , the field strength due to both windings of the coil. Therefore half of this quantity expresses the field due only to one winding. Also by regarding a and c as variables, the field strength at any point p on the y-axis due to one winding may be obtained. Now from geometry,

$$c^2 = a^2 + b^2. \text{ - - - - - (4)}$$

Accordingly, using this to substitute for c in equation (2) and dividing by 2 gives the desired magnetic field strength  $H_p$

due to one winding at any point  $p$  on the  $y$ -axis when  $a$  and  $c$  vary with the position of  $p$ . This is

$$H_p = \frac{4nIb}{a^2 + b^2} \dots (5) \text{ (e.m.u.)}$$

Differentiating this with respect to the variable  $a$  gives

$$\frac{d(H_p)}{d(a)} = 4nIb \left[ \frac{-2a}{(a^2 + b^2)^2} \right],$$

and a second differentiation gives

$$\frac{d^2(H_p)}{d(a)^2} = 8nIb \left[ \frac{4a^2}{(a^2 + b^2)^3} - \frac{1}{(a^2 + b^2)^2} \right].$$

This expression equals zero when the expression in the brackets is zero, which is easily shown to be the case when

$$a^2 + b^2 = 4a^2.$$

This requirement, using equation (4), may be written

$$c^2 = 4a^2,$$

or

$$a = \frac{c}{2} \dots (6)$$

This proportion between  $c$  and  $a$  produces the most uniform field in the center of the scanning coil. The magnitude of the field at various points on the  $y$ -axis due to each winding and due to their combined effect, when this optimum proportioning is used, is shown in Figure 14.

By using equation (4) the optimum relation of equation (6) can be expressed as a relation between  $b$  and  $c$ , the result being that  $b = (\sqrt{3}/2)c$ . Substituting this in (2) gives the field strength produced by a concentrated coil proportioned for maximum uniformity of the field, the expression being

$$H_0' = 4\sqrt{3} \frac{n}{c} I \dots (7) \text{ (e.m.u.)}$$

In practical units this is

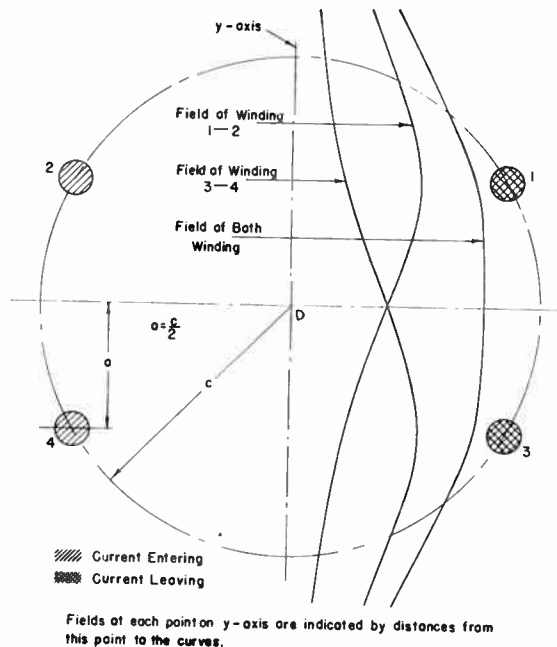


Fig. 14. Magnetic Field Due to Each Winding and Combined Field of Both for Concentrated Air-Core Coil Having Optimum Separation of Windings.

$$H_0' = 0.693 \frac{n}{c} I, \dots (8)(p)$$

- where  $H_0'$  = field strength at the center between concentrated windings having the optimum separation;
- $n$  = number of turns in each winding;
- $c$  = radius of cylinder in centimeters; and
- $I$  = current thru windings in amperes.

DISTRIBUTED TYPE OF SCANNING COIL

The scanning coil shown in Figure 2 (page 246) is made with its conductors distributed over the cylindrical surface which defines the inside of the coil. This coil can be regarded as being built up of a large number of concentrated windings. By adjusting the number of turns in the component concentrated windings according to their position along the  $y$ -axis (see Figure 13), it is possible to adjust the field-intensity distribution within the scanning zone, since this field is due to the combined effect of all the component windings.

The relation between the number of turns in these concentrated-winding components and their distance along the y-axis, which will give the most uniform field distribution in the enclosed cylindrical volume, is of practical interest, and we now consider this.

Consider an ellipsoid whose surface is covered with current-carrying wire loops, each of these loops lying in a plane and all the planes being parallel to each other. It can be shown that if these loops are so distributed that the number of ampere-turns per unit length along the normal to the planes of these loops is constant, the resultant magnetic field is uniform throughout the volume of the ellipsoid and is directed along the normal to the planes of the loops. (This is shown in the book "Leçons d'Électricité et le Magnétisme" by E. Mascart and J. Joubert, Volume 1, page 546, published in Paris in 1882.)

The cylindrical volume of the scanning zone can be regarded as the central part of a very long ellipsoid of revolution. To produce a uniform field distribution at right angles to the major axis within such a long ellipsoid requires a winding distribution such that the number of ampere-turns per unit length is constant in the direction of the field. With the same current thru all the turns, there must only be a constant number of turns per unit length in the field direction. Considering now the central part of the long ellipsoid, which is very nearly a cylinder, we see that the above principle of constant turns per unit length in the field direction gives the required winding distribution for the distributed scanning coil. An actual coil made in accordance with this rule will not have an absolutely uniform field throughout its length, and will have some fringing field, because of the neglected effect of the end turns.

Figure 13 can be taken to represent part of a distributed coil. If the number of turns per unit length in the y-direction is taken as  $n_1$ , and if the height of a small section of one winding in the same direction (the direction of the dimension  $a$ ) is taken as an

infinitesimal  $da$ , the number of turns in this section of winding will be  $n_1 da$ . From equation (2) we see that the infinitesimal differential of the total field produced at the center  $O$  by this section and the one symmetrically opposite will be given by

$$dH = \frac{8 n_1 I b}{c^2} da. \quad - - (9)(\text{e.m.u.})$$

The field produced at point  $O$  by the entire distributed coil can be determined by integrating this expression over a range of  $a$  from zero to  $c$ , the radius of the cylinder. The latter limit is chosen because the turns are distributed all the way to the top. Indicating this integration, we have

$$H = \frac{8 n_1 I}{c^2} \int_0^c b da. \quad - - (10)(\text{e.m.u.})$$

From equation (4) the value of  $b$  in terms of  $a$  is available as

$$b = \sqrt{c^2 - a^2},$$

whence

$$\begin{aligned} H &= \frac{8 n_1 I}{c^2} \int_0^c \sqrt{c^2 - a^2} da \\ &= \frac{8 n_1 I}{c^2} \times \frac{1}{2} \left[ a \sqrt{c^2 - a^2} + c^2 \sin^{-1} \frac{a}{c} \right]_0^c \\ &= \frac{8 n_1 I}{c^2} \times \frac{1}{2} \left[ \frac{\pi}{2} c^2 \right], \end{aligned}$$

$$\text{or } H = 2 \pi n_1 I. \quad - - - - (11)(\text{e.m.u.})$$

A distributed coil consists of course of two similar halves, or windings, just as a concentrated coil does. The total number of turns  $n$  in each winding of the distributed coil is equal to the turns per centimeter  $n_1$  times the height of the winding in the direction of the field. That is,

$$n = n_1 c. \quad - - - - - (12)$$

Substituting this in (11) gives the field strength within a distributed coil which

is proportioned for uniformity, the expression being

$$H = 2\pi \frac{n}{c} I. \dots (13)(e.m.u.)$$

In practical units this is

$$H = 0.628 \frac{n}{c} I, \dots (14) (p)$$

where H = field strength; oersteds

n = number of turns in each winding;

c = radius of cylinder in centimeters; and

I = current thru windings in amperes.

Equations (13) and (14) apply accurately in the case of a cylinder of infinite length. When the cylinder is finite in length they give the approximate field strength in the center. This approximation is less accurate for shorter lengths of cylinder because of the greater influence of the end portion of the winding. The values of computed deflection, assuming that a short coil produces the ideal field given by equations (13) and (14), would be expected to agree with measurements to the same degree as with concentrated coils, as described above on page 251. This is because the distributed coil can be regarded as built up of a number of concentrated coils.

TESTING OF SCANNING COILS

<sup>Storage</sup>  
Energy Factor

The function of a scanning coil is to deflect the beam. It does this by establishing at each instant the necessary magnetic field. This field represents <sup>instantaneous</sup> storage of energy received from the scanning circuits. One aim in design is to make this energy as small as possible for a given angle of deflection. It is desirable to have a number indicating the relation between magnetic field energy and deflection angle, so that different coil designs may be compared. Since the deflection angle depends upon beam voltage this factor must be taken into account.

We therefore introduce such a quantity, calling it the "energy factor for magnetic deflection", and defining it as follows:

$$q = \frac{W}{E\phi^2}, \dots (15) (p)$$

where q = energy <sup>storage</sup> factor for magnetic deflection; coulombs

W = energy in field in joules;

E = potential of beam in volts; and

φ = angle of deflection in radians.

*q has dimensions of quantity of charge*

However

$$W = \frac{1}{2} LI^2, \dots (16)(p)$$

where L = inductance of scanning coil in henries; and

I = current thru scanning coil in amperes.

Substituting this value of W in (15) gives

$$q = \frac{LI^2}{2E\phi^2}. \dots (17)(p)$$

In the preceding chapter (Report 1932, equation (34)<sup>33</sup>, page 231), a relation is given for the sine of φ in terms of the flux density. For the present purpose we may take the angle φ in radians as equal to the sine, and write H for B since the medium is vacuum, thus obtaining

$$\phi = \frac{0.30}{\sqrt{E}} H L', \dots (18)(p)$$
  
$$\phi = \frac{H L'}{\sqrt{2E}} \sqrt{\frac{e}{m}} \quad c.m.u.$$

where H = intensity of scanning field; and ~~and~~

L' = length of scanning field in centimeters.

E = potential of beam, in volts  
e = charge of electron, in coulombs m = electronic mass, grams

Equation (18) is based on the assumption that the field intensity H has a constant value over the length L' and is zero everywhere else. This expression can be generalized to take into account the fringing field, which causes H to vary gradually at the ends of the scanning coil; this may be done by integration as follows:

$$\phi = \frac{0.30}{\sqrt{E}} \int_a^b H dz, \quad \dots (19)(p)$$

$$\phi = \frac{\sqrt{e/m}}{\sqrt{2E}} \int_a^b H dz \quad \text{EMU} (!)$$

where  $z$  is measured along the electron-optical axis, and the integration limits  $a$  and  $b$  are sufficiently far away from the ends of the coil so that the field beyond these points is substantially zero.

It is possible to measure the value of the integral (19) by electrical means as illustrated in Figure 15. A pickup coil of a uniform width of  $G$  centimeters having  $n$  turns and of sufficient length to extend beyond the fringing field, is inserted in the scanning coil and placed on the axis so that the plane of the pickup coil is normal to the magnetic field produced by the scanning coil. The pickup coil and the scanning coil have a mutual inductance  $M$  which can be measured by means of the inductance bridge shown.

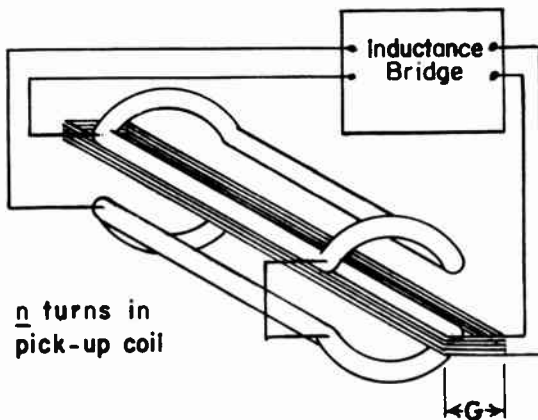


Fig. 15. Pickup Coil Used in Obtaining Values of Energy Factor  $q$  and Energy-Dissipation Factor  $p$ .

From the definition of mutual inductance, we can say that the total magnetic flux  $\phi = nN$  which threads the  $n$  turns of pickup coil when a current  $I_1$  flows in the scanning coil is given by the relation,

$$nN = MI_1, \quad n\phi = MI \quad \text{EMU}$$

or

$$N = \frac{MI_1}{n} \quad \dots \dots \dots (20)(p)$$

$$F = \frac{MI}{n} \quad \text{EMU}$$

However, in the present case the total flux  $\phi$  is also given by the relation,

$$\phi = G \int_a^b H dz. \quad \text{EMU}$$

Equating these two expressions for  $N$ , there results

$$G \int_a^b H dz = \frac{MI_1}{n},$$

or

$$\int_a^b H dz = \frac{MI_1}{Gn}.$$

Substituting this in equation (19) gives

$$\phi = \frac{0.30}{\sqrt{E}} \frac{MI_1}{Gn} = \frac{\sqrt{e/m}}{\sqrt{2E}} \frac{MI}{Gn} \quad \text{EMU}$$

$$\phi = \frac{29.7 \times 10^6}{\sqrt{E}} \frac{MI}{Gn}, \quad E \text{ in volts, } M \text{ in henries, } I_1 \text{ in amp}$$

This expression for  $\phi$  may now be substituted in equation (17) giving

$$q = \frac{LI_1^2}{2E \left( \frac{0.30}{\sqrt{E}} \frac{MI_1}{Gn} \right)^2},$$

which simplifies to

$$q = 5.56 L \left( \frac{Gn}{M} \right)^2. \quad \dots (21)(p)$$

$$q = 0.568 \times 10^{-15} L \left( \frac{Gn}{M} \right)^2$$

We see from this equation that the value of  $q$ , the energy factor, for a given scanning coil may be determined from a measurement of  $L$  the self inductance of the coil, and  $M$  the mutual inductance between the scanning coil and a long rectangular pickup coil of known width  $G$  (centimeters) and number of turns  $n$ .

Power-Dissipation Factor

At each extreme of scanning, the energy of the magnetic field,  $1/2 LI^2$ , has been transferred from the circuit to the field; during the next retrace this energy is returned to the circuit. The energy factor of the preceding section is proportional to the amount of this energy. However, the scanning coils have some resistance which produces a dissipation of power. In addition, eddy-current losses produce some power dissipation in coils which have an

iron sheath. This iron loss is usually negligible with the field scanning coil which operates at relatively low frequencies, but can be appreciable with the line scanning coil due to the high scanning frequency. It is obviously desirable to hold this power dissipation to a minimum. As a figure for comparing scanning coils with respect to the total dissipation in the coil, we now define a quantity  $p$ , calling it the "power dissipation factor for magnetic deflection", its value being as follows:

$$p = \frac{I^2 R}{E \phi^2}, \quad \text{--- (22)(p)}$$

where  $p$  = power-dissipation factor for magnetic deflection; *amp.*

$I$  = scanning-coil current in amperes;

$R$  = effective resistance of scanning coil in ohms;

$E$  = potential of cathode-ray beam in volts; and

$\phi$  = angle of deflection of beam in radians.

Using this relation and equation (17), the ratio of  $p$  to  $q$  is found to be

$$\frac{p}{q} = \frac{I^2 R}{E \phi^2} \left( \frac{2 E \phi^2}{L I^2} \right) = \frac{2 R}{L}.$$

From this

$$p = \frac{2 R q}{L}.$$

Substituting for  $q$  from equation (21), there results

$$p = 11.12 R \left( \frac{G n}{M} \right)^2, \quad \text{--- (23)(p)}$$

$$p = 1.14 \times 10^{-15} R \left( \frac{G n}{M} \right)^2$$

where  $G$  = width of pickup coil in centimeters;

$n$  = number of turns in pickup coil; and

$M$  = mutual inductance in henries between scanning and pickup coils.

This equation shows that the value of  $p$  for a given scanning coil can be determined from a measurement of the resistance of the coil and a measurement of the mutual inductance between the scanning and pickup coils in a way similar to that used for determining  $q$ .

In the design of scanning coils, the relative importance of the factors  $p$  and  $q$  depends upon the scanning frequency. For the line scanning coil, which operates at a high frequency, it is desirable to keep the energy factor  $q$  as low as possible, whereas for the field scanning coil it is desirable to keep the energy-dissipation factor  $p$  as low as possible.

Table I gives values of  $q$  and  $p$  for a number of different types of scanning coils. These were determined by the method described, the mutual-inductance measurements being made at a frequency of 1000 cycles. In computing the value of  $p$ , the direct-current resistance was used, whence a slight error is present. For high accuracy  $R$  would have to be measured with sawtooth current of a chosen retrace fraction and amplitude. The last two columns in the table give a few values of  $q$  obtained from observation of the deflection  $\phi$  for a given scanning current  $I$ , using equation (17).

Yoke number 4, as shown in the table, did not have an iron sheath. This yoke was subsequently covered with an iron-wire sheath and identified as yoke No. 4'. It can be seen from the table that the addition of the iron sheath reduced, that is improved, the  $p$  and  $q$  values for both horizontal and vertical deflection. The same holds true for yokes 5 and 5' where also an iron-wire sheath was added.

It should be noted that a comparison of the  $p$  and  $q$  values between different yokes is only valid if the coils have the same length. In general the  $p$  and  $q$  values are smaller, that is better, for the longer coils.

#### Measurement of Field Intensity

The role of the fringing field in producing defocusing of the scanning

TABLE I

VALUES OF ENERGY FACTOR  $q$  AND ENERGY-DISSIPATION FACTOR  $p$   
FOR LINE AND FIELD COILS OF SEVERAL YOKES

Yoke Number	Overall Coil Length in Inches	Type of Winding	Type of Sheath	D-C Resistance in Ohms		Inductance in Millihenries		Value of $p$ in Trillions Using Pickup Coil -- Equation (23)		Value of $q$ in Billions Using Pickup Coil -- Equation (21)		Value of $q$ in Billions from Beam Deflection -- Equation (17)	
				H	V	H	V	H*	V	H	V	H	V
1	3-1/4	Nested	Iron Wire	5.10	4480	1.51	5070	<del>9.2</del> 0.92	<del>4.0</del> 0.4	<del>1.4</del> 0.14	<del>2.3</del> 0.23	<del>1.1</del> 0.11	<del>1.9</del> 0.19
2	3-1/4	Nested	Iron Wire	5.23	42.8	1.50	40.4	<del>10</del> 1.0	<del>5.2</del> 0.52	<del>1.5</del> 0.15	<del>2.5</del> 0.25		
3	1-3/4	Slotted		3.72	876	1.66	829	<del>7.0</del> 0.7	<del>3.0</del> 0.3	<del>1.6</del> 0.16	<del>1.4</del> 0.14		
4	3-3/4	Concentrated	None	3.10	6060	1.38	7500	<del>7.6</del> 0.76	<del>4.8</del> 0.48	<del>1.7</del> 0.17	<del>3.0</del> 0.30	<del>1.4</del> 0.14	<del>2.6</del> 0.26
4'	Same coil as #4		Iron Wire	3.10	6060	1.66	10,400	<del>4.6</del> 0.46	<del>2.2</del> 0.22	<del>1.2</del> 0.12	<del>1.9</del> 0.19		
5	2-1/8	Concentrated	None	2.70	5720	1.21	6300	<del>10</del> 1.0	<del>14</del> 1.4	<del>4.0</del> 0.40	<del>7.8</del> 0.78	<del>3.6</del> 0.36	<del>7.4</del> 0.74
5'	Same coil as #5		Iron Wire	2.70	5720	1.38	7850	<del>12</del> 1.2	<del>7.1</del> 0.71	<del>2.9</del> 0.29	<del>4.9</del> 0.49		
6	2	Concentrated	Laminated	5.19	6.07	1.72	2.73	<del>11</del> 1.1	<del>10</del> 1.0	<del>1.8</del> 0.18	<del>2.3</del> 0.23		

H = Horizontal or Line Coil.

V = Vertical or Field Coil.

All yokes have inside diameter of 1-1/2" for line scanning coils.

Field scanning coils wound on outside except with yoke #3.

\* Using d-c resistance, iron loss at line frequency may increase these figures substantially.

spot is discussed in the preceding chapter, Report 1932, page 240. A treatment of this subject is also available in the volume, "Electron Optics in Television", by Maloff and Epstein, pages 204-207.

In the design of scanning coils it is necessary therefore to consider defocusing effects, as well as to obtain good efficiency, the latter requiring low

values of  $p$  and  $q$ . In order to study the uniformity of the field it is necessary to explore it with some measuring device. For this purpose a small pickup coil can be employed. This may well consist of a small flat coil oriented at right angles to the direction of the field. Measurements using this coil can be made by any one of the following three methods:

(1) The pickup coil is connected to a tube voltmeter and the scanning coil is excited with a steady sine-wave alternating current of some convenient constant frequency. Voltages indicated by the tube voltmeter are proportional to the field intensity at various positions of the pickup coil.

(2) The mutual inductance between the pickup coil and the scanning coil is measured with an inductance bridge. These values of mutual inductance are proportional to the field intensity at the various positions where the pickup coil is placed.

(3) The pickup coil is connected to a ballistic galvanometer, and a direct current is sent thru the scanning coil and adjusted to a steady value. By means of a reversing switch the current in the scanning coil is suddenly reversed, thus producing a flow of electrical charge thru the pickup coil, which is measured by the ballistic galvanometer. The field intensity at the pickup coil can then be determined from the relation,

$$H = \frac{2QR}{Sn}, \dots (24)(p)$$

- where H = magnetic field strength;
- Q = charge flowing thru the pickup coil in coulombs;
- R = resistance of pickup coil and galvanometer circuit in ohms;
- S = area of opening in the pickup coil in square centimeters; and
- n = number of turns in pickup coil.

It should be noted that in all these measuring methods, the average value of the magnetic flux over the area of the pickup coil is the quantity actually measured. The "resolving power" of the method therefore depends on the coil size and becomes greater as the coil is diminished.

Measurement of Sawtooth Currents

The peak-to-peak swing of the sawtooth scanning current is the value

generally used, and is indicated as  $I_s$  in Figure 16. This may be measured directly from the waveform as observed on an oscilloscope screen. It is more convenient, however, to measure it with an alternating-current meter.

An ordinary alternating-current meter, such as a thermal type, measures the quadratic-mean (root-mean-square) value of the current passing thru it. It is easy to show that the root-mean-square current  $I_{ac}$  of an ideal sawtooth form is related to the peak-to-peak value  $I_s$  as follows:

$$I_{ac} = \frac{I_s}{\sqrt{12}} = 0.289 I_s. \dots (25)$$

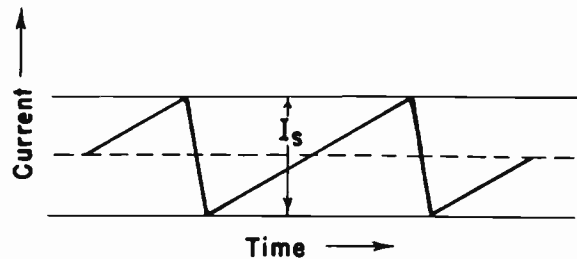


Fig. 16. Sawtooth Current Wave Showing Peak-to-Peak Value.

A rectifier type of alternating-current meter, however, responds to the average value of the rectified current passing thru it. This is a type limited in frequency range because of the inductance of the moving coil. If such a meter were calibrated to read the average rectified current, it would read one-fourth of the peak-to-peak sawtooth current. But, as a rule, rectifier-type instruments have the scale calibrated to read the r-m-s value of a sine-wave current. The average rectified value of a sine-wave current is  $\sqrt{8}/\pi$  times the r-m-s value. Therefore, when such a meter is used for measuring a sawtooth current, the reading is the r-m-s value of a sine-wave current whose rectified average value is equal to the rectified average value of the sawtooth current. Let the reading on the meter be  $I'_{ac}$ ; then

$$\frac{\sqrt{8}}{\pi} I'_{ac} = \frac{I_s}{4},$$

the left side being the average of the sine-wave current and the right side the

average of the sawtooth current. Solving this for the desired peak-to-peak sawtooth current  $I_s$ , there results

$$I_s = \frac{\sqrt{128}}{\pi} I'_{ac} = 3.60 I'_{ac}. \quad (26)$$

From equations (25) and (26), a total of six relations between the three figures for a sawtooth current can be obtained; these are as follows:

$$I_s = \sqrt{12} I_{ac} = 3.46 I_{ac}; \quad (27)$$

$$I_{ac} = \frac{1}{\sqrt{12}} I_s = 0.289 I_s; \quad (28)$$

$$I_s = \frac{\sqrt{128}}{\pi} I'_{ac} = 3.60 I'_{ac}; \quad (29)$$

$$I'_{ac} = \frac{\pi}{\sqrt{128}} I_s = 0.278 I_s; \quad (30)$$

$$I_{ac} = \frac{8}{\pi \sqrt{6}} I'_{ac} = 1.04 I'_{ac}; \quad (31)$$

and

$$I'_{ac} = \frac{\pi \sqrt{6}}{8} I_{ac} = 0.96 I_{ac}. \quad (32)$$

These six relations are based on certain assumptions, and hold accurately only when these are fulfilled. These assumptions are:

(1) The wave has a linear sawtooth shape on the trace and relatively small duration of retrace;

(2) The meter responds correctly to current components of a sufficiently wide frequency range; and

(3) In the case of the rectifier meter, the current thru the meter follows the rectified waveform.

The ordinary rectifier type of milliammeter is accurate only at the lower frequencies and therefore is suitable for measuring current of the field frequency but not of the line frequency.

On the other hand, a high-frequency alternating-current ammeter, say of the thermal type, is suitable for measuring current of either field or line frequency.

In practice, the rectifier type of meter does not operate with perfect rectification, especially on small currents where the scale is non-linear and the operation approaches that of an r-m-s meter. The error from this cause is less than 4 percent (and usually of the order of one percent) in the measurement of sawtooth currents with a meter calibrated for sine-wave currents, as seen in equations (31) and (32). This error is small because the sawtooth waveform is somewhat similar to a sine waveform.

The magnetic field energy and the power loss in terms of the three current figures are as follows:

$$W = \frac{L(I_{ac})^2}{2} = \frac{L I_s^2}{24} = \frac{16}{3 \pi^2} (I'_{ac})^2, \quad (33)$$

and

$$P = R(I_{ac})^2 = \frac{R I_s^2}{12} = \frac{32}{3 \pi^2} (I'_{ac})^2. \quad (34)$$

The notation in these and the other equations of this section is as follows:

$I_s$  = peak-to-peak current swing of sawtooth wave;

$I_{ac}$  = root-mean-square value of sawtooth wave;

$I'_{ac}$  = reading of rectifying type of meter on sawtooth wave;

$W$  = average energy in magnetic field of scanning coil;

$P$  = average power dissipation in scanning coil;

$L$  = inductance of scanning coil; and

$R$  = resistance of scanning coil.

#### Testing for Uniformity of Scanning Speed

It is assumed that at the transmitter the scanning of the picture takes

place at a perfectly uniform rate. That is, the scanning spot in its progress from one side to the other, proceeds at a strictly constant speed, and similarly the vertical scanning, from the top of the scene to the bottom, also is at a perfectly constant rate. On this basis the desired operation at the receiver is to achieve a similar uniformity in the scanning speed for both the horizontal and vertical scanning.

If the scanning spot in its horizontal motion does not have uniform speed, an object will be reproduced with a varying width as it moves to different positions in the picture. In case the camera is turned slowly so as to give a passing panoramic view, a given object is seen in various parts of the field of view and the disconcerting effect is noticed that the apparent size of the object changes with its position in the field. A similar effect would be noticed with the vertical scanning if the camera were steadily pointed more and more upward or downward, but this is seldom done. In this way, a changing speed of the scanning spot appears to the eye as a changing width or height of a given object in different parts of the field of view.

In the preceding chapter, Report 1932, pages 229-231, there is derived the relation that the sine of the angle of deflection is proportional to the magnetic deflecting field. For wide-angle tubes the departure of the sine of an angle from proportionality to the angle itself becomes appreciable. For simplification, the present discussion is limited to moderate angles for which the sine can be considered as proportional to the angle. On this basis the desired uniformity of scanning speed can be obtained if the magnetic flux follows a linear sawtooth variation during the trace portion of the cycle. The flux may of course follow any curve during retrace because none of the picture is being reproduced during this time.

Any deviation from the linear sawtooth wave of magnetic field intensity introduces, as noted above, a geometrical distortion in the reproduced image. On account of the importance of this effect

there is a need for means of detecting or measuring this deviation. In the present section three methods for testing the uniformity of scanning speed are described.

One method of testing the uniformity of slope of the trace portion of the line scanning wave consists in operating the picture tube with line and field scanning and modulating the grid with a square wave of a frequency which is a moderately high harmonic of the line frequency. In this way a pattern of vertical bars is produced on the screen. The uniformity of spacing in this fixed pattern is a measure of the uniformity of the sawtooth slope, or linearity of the line scanning. A corresponding test can be used for the vertical field scanning.

Another method consists in observing the current waveform with an oscilloscope. In the case of the line scanning the current may be passed thru a small resistor without appreciable change of the waveform. The voltage drop across this resistor is amplified as much as necessary and applied to a cathode-ray oscilloscope, which then shows the current waveform. If the oscilloscope trace frequency is adjusted to 4410 cycles, which is one-third of the line frequency of 13,230 cycles, three cycles of the sawtooth wave, as shown in Figure 17-A, will be observed. If the oscilloscope trace frequency is adjusted to two-thirds of the line frequency, that is to 8810 cycles, a pattern such as is shown in Figure 17-B will be observed. The exponential curvature of the wave can readily be detected in this drawing by the departure from parallelism between one part of one trace  $S_1$  and another part of another trace  $S_2$ .

The waveform of the sawtooth current in the field scanning coil may likewise be observed with a cathode-ray oscilloscope. The impedance of the field scanning coil to the field-frequency sawtooth current is mostly resistive. The voltage across this coil may be amplified and applied to the oscilloscope, which will then indicate the current, accompanied by a pulse component of voltage due to the inductance. If the oscilloscope trace frequency is adjusted to 20

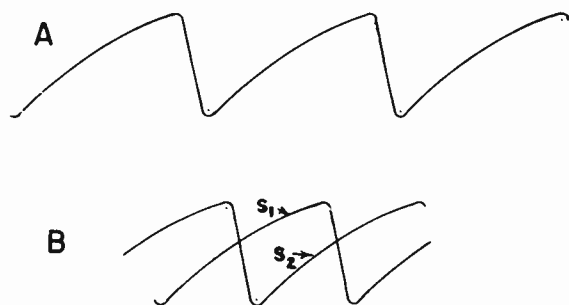


Fig. 17. Check of Line Scanning Linearity by Parallelism of  $S_1$  and  $S_2$  Using 8810-Cycle Oscilloscope Trace Frequency.

cycles, three of the scanning waves will be observed, as in Figure 18-A. By using a frequency of 420 cycles for the oscilloscope trace, each cycle of Figure 18-A will in effect be divided into 7 equal segments along the time axis, and a pattern such as Figure 18-B will be observed on the oscilloscope. This pattern has advantages over the preceding in that the retrace time may be more accurately measured and any departure from linearity of the trace may be more readily noted. The departure from linearity is shown by failure of parallelism, assuming that the oscilloscope trace is linear. If it is not desired to rely on the oscilloscope linearity, the departure of the tested wave from linearity can be noted by the inequality in the division of a vertical line, as indicated in the drawing.

It should be noted that in general the reliability of waveform measurements made with an oscilloscope depends on the fidelity of the oscilloscope amplifier and on the sweep linearity of the oscilloscope. With the overlapping methods of Figures 17-B and 18-B the dependence on the oscilloscope linearity is less critical or absent, which is another advantage of these methods.

The sensitivity of measurement of the linearity of a sawtooth waveform can be greatly increased by observing on the oscilloscope not the wave itself, but

its slope or first derivative with respect to time. By a consideration of several types and amounts of scanning distortion it can be seen that the departure of the slope wave from flatness (constancy) during the trace is representative of the severity of the distortion as seen by the observer. This is in agreement with the fact already noted that non-uniformity of scanning speed causes variation in the size of a given object in various parts of the field of view. This agreement will be realized on noting that the scanning speed is given by the height of the slope wave. As an example of these statements, the width of an object seen on the picture tube is proportional to the horizontal scanning speed in that part of the picture.

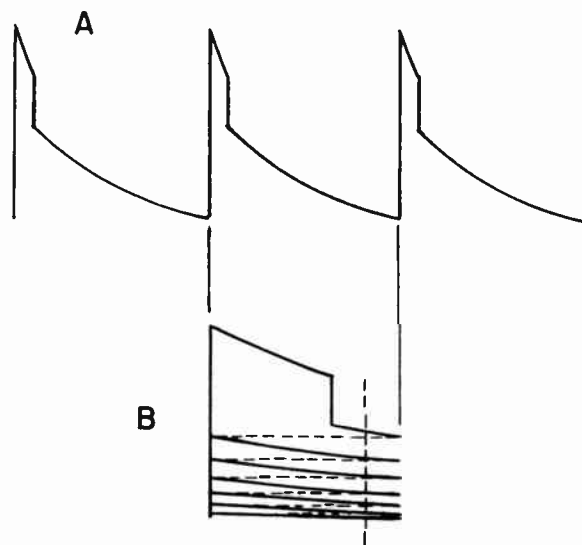


Fig. 18. Check of Field Scanning Linearity by Intercepts on Vertical Line Using 420-Cycle Oscilloscope Trace Frequency.

Variation in scanning speed also causes variation of picture brightness. Where the speed is too high, the brightness is of course less than it should be, and vice versa. The sawtooth wave may contain slight ripples which cannot be seen in a direct oscilloscopic examination, but which are sufficient to produce perceptible non-uniformity in a

flat picture background; the presence of such ripples is readily seen in a slope-wave examination.

The slope of the sawtooth wave of Figure 19-A is shown in Figure 19-B. The parts of the curve of Figure 19-B which are above the axis correspond to the traces of the sawtooth wave and are the only parts which are of interest in connection with the linearity of scanning. It is desirable to clip off the narrow pulses of the curve below the axis, which occur during retrace, so that the full amplitude of the oscilloscope may be used to observe the upper parts of the curve.

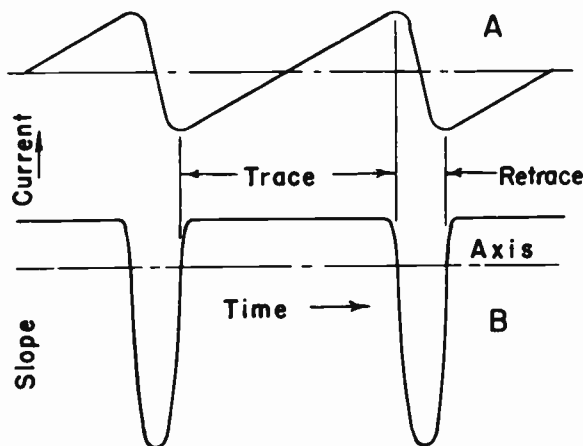


Fig. 19. Sawtooth Current Wave and the Corresponding Slope Wave.

The instants at which the slope curve crosses the axis mark the points of zero slope, or maximum excursion, of the sawtooth wave, and therefore define accurately the transition from trace to retrace and vice versa. It is at these instants of time that the scanning spot is momentarily stationary before reversing its direction of travel. To obtain these accurately it is necessary to know the position of the axis of the slope wave. Another advantage resulting from the knowledge of the position of the axis is that it serves as a reference; in particular it represents the zero value of scanning speed. The clipping circuit described below operates to clip at the zero of the slope wave, and therefore gives these advantages.

The slope wave can be obtained by means of a pickup coil which is placed inside the scanning coil. The potential  $E$  in volts induced in this pickup coil is given by

$$E = - M \frac{dI}{dt}, \quad \text{--- (35)(p)}$$

where  $M$  = mutual inductance in henries between scanning coil and pickup coil;

$I$  = current thru scanning coil in amperes; and

$t$  = time in seconds.

A circuit which can be used for clipping the retrace peaks from the derivative voltage wave induced in the pickup coil is shown in Figure 20. The pickup coil is connected with such polarity that during trace the input terminal  $A$  is negative, the upper diode is closed, and the lower diode is open, so that the full voltage induced in the pickup coil appears across resistor  $R$  and is applied to the grid of the amplifier tube. During retrace the voltage on terminal  $A$  is positive, the upper diode is open, and the lower diode is closed, so that all the voltage is developed across the upper diode, the voltage across  $R$  being zero. This resistor is shorted by the lower diode, and therefore there is no input to the amplifier during retrace. This action causes the circuit to clip the input voltage at zero, so that the height of the resultant output wave is proportional to the slope of the sawtooth wave. The clipped wave appearing across the output terminals  $A'$  and  $B'$  is applied to an amplifier, and the amplified voltage wave is observed on the oscilloscope screen.

This method is of great utility in studying line scanning coils and circuits under operating conditions since it is convenient and simple to use, and does not require a picture tube.

It should be noted that to avoid waveform distortion the capacitance and inductance of the pickup coil should

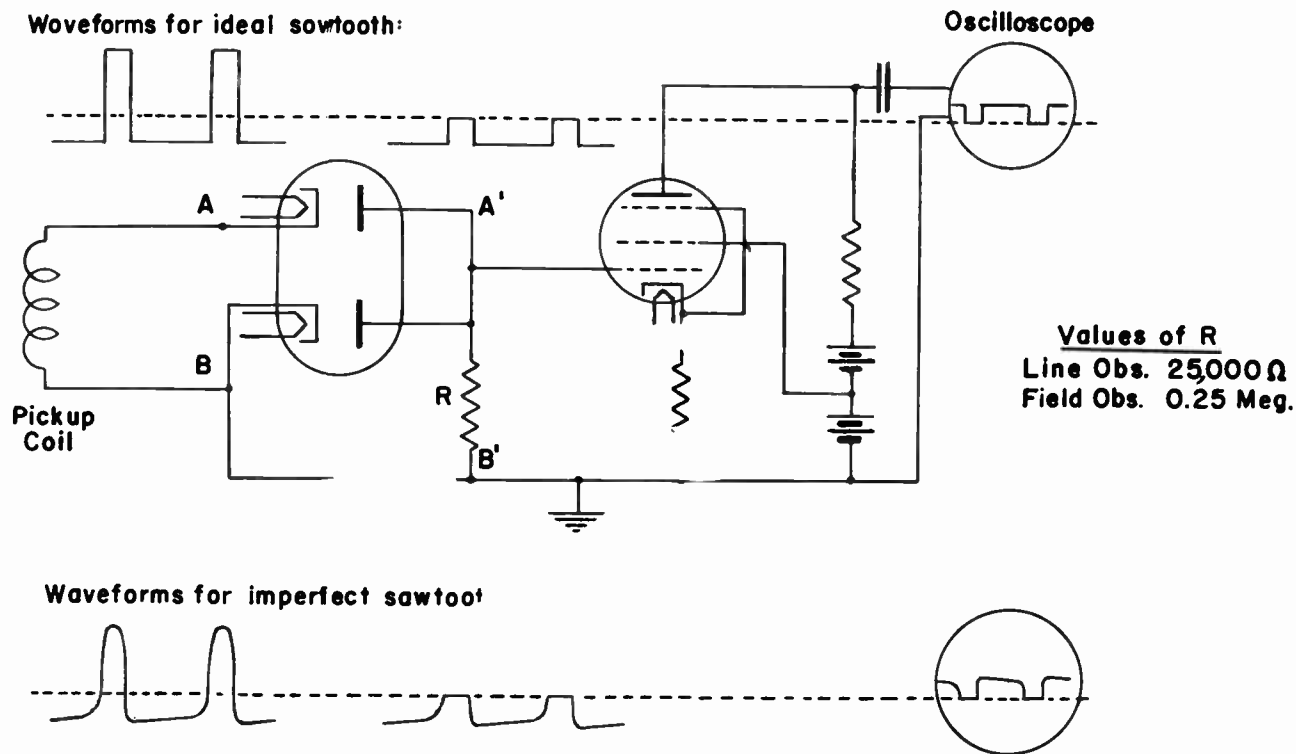


Fig. 20. Circuit for Clipping the Slope Wave at Its Axis.

not be too great, and the free oscillations may have to be damped. This pickup coil can be similar to that of Figure 15, except that in the case of the line coil electrostatic shielding may be needed.

A discussion of the use of the slope wave for studying scanning-wave distortion is given in RCA License Bulletin LB 473, "A New Method for Determining Sweep Linearity", by S. W. Seeley and C. W. Kimball. The circuit described therein differs somewhat from the one presented here.

TRANSFORMERS FOR SCANNING COILS

Reasons for Using a Transformer

The sawtooth current which drives a scanning coil can be supplied directly, or thru a transformer, from the plate of a vacuum tube which is operating in a suitable circuit. There are a

number of such circuits, and these will be described in a later chapter.

A scanning coil which is designed to have an optimum load inductance for use directly in the plate circuit of the amplifier tube requires a large number of turns of wire. For line scanning coils the necessary inductance is of the order of 50 millihenries. Such direct connection requires special consideration in regard to the following limitations which are often encountered:

(1) The self capacitance of the scanning coil and its leads makes the natural frequency too low and places a limit on the speed of retrace;

(2) The voltage developed during retrace is very high (several thousand volts), and consequently the insulation of coils and leads must be given special attention; and

(3) Capacitive coupling between line and field scanning coils may induce line-frequency disturbances in the field deflection, impairing the interlace.

These limitations are reduced by using a transformer to couple the line scanning coil with the vacuum-tube circuit. This frees the coil design from impedance limitations imposed by the vacuum-tube characteristic. In this way it is possible to design the line scanning coil with inductance which is only a small fraction of that required for a direct connection. The number of turns in the coil is thereby very much reduced. This change in coil design reduces each of the limitations listed in the preceding paragraph. For example, if the inductance of the line scanning coil is decreased to  $1/25$ , the following results are obtained:

(1) The natural frequency is multiplied by 5, and therefore the lower limit of the retrace time is decreased to  $1/5$ ;

(2) The voltage developed across the coil during retrace is decreased to  $1/5$ ;

(3) The energy transferred by the capacitive coupling from the line scanning coil to the field scanning coil is decreased to  $1/5$ ; (if the inductance of the field scanning coil were likewise reduced by the same factor, the energy transferred by capacitive coupling between line and field scanning coils would be reduced to  $1/25$ ); and

(4) The number of turns is reduced to  $1/5$  and the wire diameter increased by  $\sqrt{5}$ ; (this latter point is of greater importance for field scanning coils, which have a larger number of turns, since a more rugged and cheaper coil can thus be used).

The line scanning coils of all the yokes listed in Table I on page 257 are designed for driving from a transformer. The inductance values can be seen to lie in the range from 1.2 to 1.8 millihenries.

### Design of Line-Frequency Transformers

The present section, and the following ones on attenuation, efficiency, and resistance, give a discussion of the more unusual aspects which characterize the design of transformers for line scanning.

Figure 21 shows the circuit of a line scanning coil which is coupled thru a step-down transformer with the driving amplifier. In this case the load inductance  $L_c$  is a limiting factor. We shall show that on account of this inductive load the transformer must have nearly unity coupling  $k$  in order to transfer energy efficiently. In addition, the transformer must be carefully designed to match its load and to present the proper inductance as a load on the amplifier tube. Also the shunt capacitance, especially in the primary winding, must be kept to a minimum.

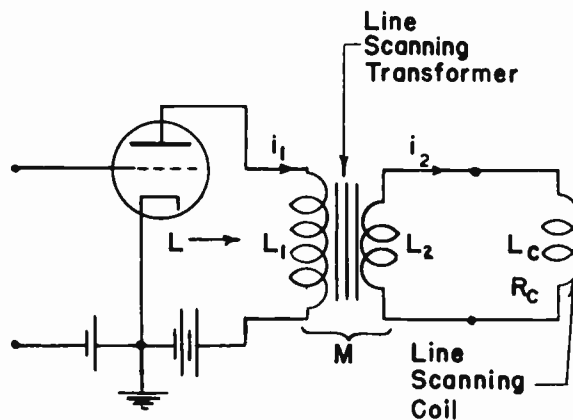


Fig. 21. Line Scanning Transformer Between Tube and Line Scanning Coil.

The coefficient of coupling  $k$  of the transformer of Figure 21 is given by the well-known relation,

$$k = \frac{M}{\sqrt{L_1 L_2}}, \quad \text{--- (36)}$$

- where  $M$  = mutual inductance between primary and secondary;
- $L_1$  = self inductance of primary (measured with secondary on open circuit);
- $L_2$  = self inductance of secondary (measured with primary on open circuit).

The T-type equivalent circuit of the scanning transformer of Figure 21 is shown in Figure 22. This is seen to be an attenuator with inductive arms. Such an attenuator, when connected with an inductive load, can be shown to have least attenuation when the load inductance  $L_c$  matches the secondary image inductance. Under this condition, the transformer should present on the primary side an apparent inductance  $L$  which has a certain optimum value depending on the vacuum-tube characteristics and type of operation.

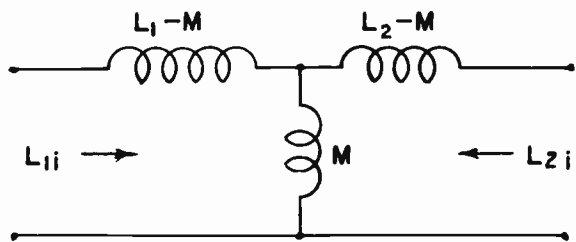


Fig. 22. Equivalent Circuit of Line Scanning Transformer.

The image impedance at one side of a four-terminal network is the geometric mean of the two impedance values which the network has on this side when the opposite side is respectively short-circuited and open-circuited. For the network of Figure 22 these impedances are all inductances so the rule just stated can be expressed for the left-hand side in the following way:

$$L_{1i} = \sqrt{L_{1sc} L_1} \dots \dots \dots (37)$$

The ratio of the short-circuit inductance to the open-circuit inductance

is the same on the primary and secondary sides, so that in this ratio it is not necessary to use subscripts. We now show that this ratio bears a simple relation to the coefficient of coupling. Considering the left-hand side of Figure 22, it can be shown that

$$\frac{L_{sc}}{L_{oc}} = \frac{(L_1 L_2 - M^2)/L_2}{L_1} = 1 - \frac{M^2}{L_1 L_2}$$

The second term here is the square of the coefficient of coupling, according to equation (36); making the substitution there results

$$\frac{L_{sc}}{L_{oc}} = 1 - k^2, \text{ or } k = \sqrt{1 - \frac{L_{sc}}{L_{oc}}} \dots (38)$$

The ratio  $L_{sc}/L_{oc}$  for the transformer can be conveniently measured on a 1000-cycle bridge. With the iron core there are hysteresis and eddy-current effects which depend on the waveform. A direct magnetization, corresponding to the plate current of the tube for which the transformer is designed, should be present during the test. The measuring signal for the open-circuit inductance should produce a very small flux density, so as to approximate the minimum inductance value as the flux is decreased. The test for short-circuit inductance is nearly independent of the core and therefore of the flux density.

The image inductance  $L_{1i}$  looking into the left-hand terminal of Figure 22 is given by equation (37) as

$$L_{1i} = \sqrt{L_{1sc} L_1},$$

whence

$$L_{1i} = L_1 \sqrt{\frac{L_{1sc}}{L_1}}$$

The fraction here is the ratio of short-circuit to open-circuit inductance at the left-hand terminals. Since this is the same on either side, we can write

$$L_{1i} = L_1 \sqrt{\frac{L_{sc}}{L_{oc}}} = L_1 \sqrt{1 - k^2} \quad (39)$$

Similarly for the right-hand terminals of Figure 22, that is for the secondary side

$$\begin{aligned} L_{2i} &= \sqrt{L_{2sc} L_2} \\ &= L_2 \sqrt{\frac{L_{sc}}{L_{oc}}} = L_2 \sqrt{1 - k^2} \quad (40) \end{aligned}$$

Equation (39) may now be applied to the primary side of the transformer of Figure 21, for which purpose we set

$$L_{1i} = L = L_1 \sqrt{\frac{L_{sc}}{L_{oc}}},$$

from which

$$L_1 = L \sqrt{\frac{L_{oc}}{L_{sc}}} \quad (41)$$

Similarly with the secondary side,

$$L_{2i} = L_c = L_2 \sqrt{\frac{L_{sc}}{L_{oc}}},$$

from which

$$L_2 = L_c \sqrt{\frac{L_{oc}}{L_{sc}}} \quad (42)$$

Attenuation of Line Transformer

The attenuation, as a current ratio, is expressed as the actual output current divided by that from an ideal transformer of the same inductance ratio. Considering the line scanning transformer, Figure 23 shows the equivalent T of Figure 22 with its output terminals connected to an inductance which matches the image inductance. The ratio of output current  $i_2$  to shunt current  $i_3$  can be expressed as follows by using equation (40):

$$\frac{i_2}{i_3} = \frac{M}{L_2 - M + L_2 \sqrt{1 - k^2}}$$

The ratio of output current  $i_2$  to input current  $i_1$  is given by

$$\frac{i_2}{i_1} = \frac{i_2}{i_3 + i_2} = \frac{M}{L_2(1 + \sqrt{1 - k^2})}$$

Substituting for  $M$  from equation (36) gives

$$\frac{i_2}{i_1} = \frac{k}{1 + \sqrt{1 - k^2}} \sqrt{\frac{L_1}{L_2}} \quad (43)$$

Of the two factors in this equation, the second is for an ideal transformer and the first is the attenuation.

Efficiency of Line Transformer

The efficiency of the line scanning transformer of Figure 21 is the ratio of the magnetic energy in the output coil, which is the scanning coil, to the total magnetic energy in transformer and output coil. From equations (41), (42), and (43) we can express this energy ratio or efficiency  $F$  as follows:

$$\begin{aligned} F &= \frac{i_2^2 L_c}{i_1^2 L} = \left( \frac{k}{1 + \sqrt{1 - k^2}} \right)^2 \\ &= \frac{1 - \sqrt{1 - k^2}}{1 + \sqrt{1 - k^2}} = \frac{1 - \sqrt{\frac{L_{sc}}{L_{oc}}}}{1 + \sqrt{\frac{L_{sc}}{L_{oc}}}} \quad (44) \end{aligned}$$

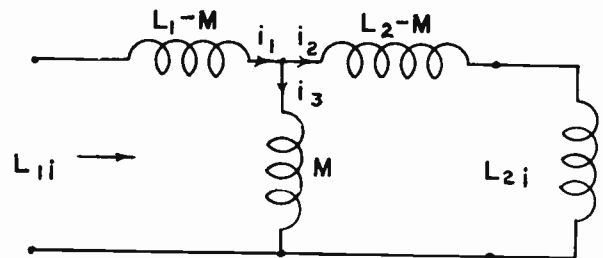


Fig. 23. Equivalent Circuit of Line Scanning Transformer with Matching Inductance Load.

### Resistance in Line-Transformer Circuits

The resistance  $R_c$  of the scanning coil is reflected into the primary circuit as a resistance  $R'$  which may be obtained by multiplying  $R_c$  by the inductance ratio and the efficiency. Thus

$$R' = R_c \frac{L_1}{L_2} F. \quad \text{--- (45)}$$

This is valid at frequencies where the resistance is much less than the inductive reactance.

The presence of the resistance  $R_c$  of the scanning coil in the closed secondary circuit causes some distortion of the current waveform. This may be corrected by adjusting the waveform of the input voltage on the grid of the amplifier tube. The apparent shunt resistance of the transformer caused by iron loss also may produce distortion of the waveform. If so, the iron loss should be made small by using very thin core laminations and a sufficient volume of iron.

The series resistance of the secondary coil may be more detrimental to efficient operation than is the resistance of the primary. If so, the secondary coil should occupy the major part of the winding space and should be on the inside next to the core. The primary has a relatively large inductance and a relatively large number of turns. It is subjected to the same capacitive effects as a directly coupled scanning coil and therefore should be sectionalized or otherwise carefully designed to minimize this capacitance.

### Field-Frequency Transformer

For the field-frequency deflection, the frequencies of the sawtooth-wave components lie in the range from 60 to say 900 cycles, at which the load impedance is mainly resistive, so that the general problem is much more like that in audio-frequency practice than is the case with line-frequency transformers.

To obtain good efficiency in field scanning transformers requires more emphasis on low resistance of the windings. This is in distinction to line scanning transformers, for which closeness of coupling is the main requirement, the efficiency depending mainly on the coupling, in the manner shown by equation (44). The greater power factor of the load in the case of the field transformer makes the efficiency higher under the usual conditions.

The field transformer affects the waveform more than the line transformer. From this standpoint reactance is important.

Of the yokes in Table I those numbered 2 and 6, with field-coil resistances of 42.8 and 6.07 ohms respectively, are designed for operation with field scanning transformers. Number 3, with a field-coil resistance of 876 ohms, may be operated either directly or with a transformer. Numbers 1, 4, and 5, with resistances of 4480, 6060, and 5720 ohms respectively, are designed for operation directly from the driving tube.

### EFFECT OF HYSTERESIS IN IRON

A reduction of speed at the beginning of the trace, caused by hysteresis, has been noticed in our laboratory in the case of line scanning with yokes having iron-wire sheaths. This is ascribed to the low value of permeability at the beginning of the hysteresis loop. The effect can probably be reduced by increasing the amount of iron.

### REFERENCES

The literature on scanning is very limited, so that only a few references can be given. These are arranged chronologically.

"Applications of the Cathode Ray Oscillograph", R. R. Batcher, PROCEEDINGS OF THE INSTITUTE OF RADIO ENGINEERS, December 1932, pages 1878-1891; an early paper including treatment of scanning coils.

"The Cathode Ray Tube in Television Reception", I. G. Maloff, RCA Manufacturing Company, PROCEEDINGS OF RADIO CLUB OF AMERICA, October 1935, pages 31-36; also in Volume I of TELEVISION, the bound RCA reprints, pages 337-354. Note sections in latter part of the paper.

"Electron Optics in Television", I. G. Maloff and D. W. Epstein, both of RCA Manufacturing Company, published by McGraw-Hill Book Company, 1938. Pages 8 and 273-277 relate to scanning yokes.

"Die Ablenkung des Elektronenstrahls in Braunschen Röhren mittels magnetischer Spulenfelder" ("The Deflection of Electron Rays in Braun Tubes by Means of Magnetic Coil Fields"), by Herbert Bähring in FERNSEH A.G., the house organ of Fernseh Aktiengesellschaft, Berlin, December 1938, pages 15-19 or (re-numbered) 51-55.

"Erzeugung sägezahnförmiger Ströme zur magnetischen Strahlablenkung in

Fernsehröhren" ("Production of Sawtooth-Shaped Currents for Magnetic Ray Deflection in Television Tubes"), Johannes Günther of Fernseh Aktiengesellschaft, Berlin, in FERNSEHEN UND TONFILM section of FUNKTECHNISCHE MONATSHEFTE, March 1939, pages 17-22.

"A New Method for Determining Sweep Linearity", S. W. Seeley and C. N. Kimball, RCA License Bulletin LB-473, March 31, 1939; discusses use of slope wave.

"Transformator-Kippgeräte", ("Transformer Scanning Apparatus"), by Theodor Mulert and Herbert Bähring in FERNSEH A.G., April 1939, pages 82-88.

"Rasterformen bei doppeltmagnetischer Ablenkung des Elektronenstrahles in Weitwinkel-Kathodenstrahlröhren", ("Raster Forms with Double Magnetic Deflection of the Electron Beam in Wide-Angle Cathode-Ray Tubes"), Johannes Günther in FERNSEH A.G., April 1939, pages 88-94.

\* \* \* \* \*

